EQA - International Journal of Environmental Quality
ISSN 2281-4485 - Vol. 73 (2026): 1 - 12
Journal homepage: https://eqa.unibo.it/

published by

Treatment of Sunset Yellow–contaminated water using biochar produced from green algae

Manel Abdallah Touati [1], Goussem Mimanne [1, 2*], Hayat Mokdad [1,3] , Karim Benhabib [2]

[1] Laboratory of materials and catalysis, Department of Chemistry, Faculty of Exact Sciences, Djillali Liabes University of Sidi Bel Abbes, Algeria
[2] Eco-Processes, Optimization and Decision Support (EPROAD, EA), University of Picardie Jules Verne - IUT of Aisne, Saint-Quentin, France
[3] Department of Analytical Chemistry, Faculty of Sciences, Saad Dahlab Blida 1 University, Blida, Algeria

* Corresponding author E.mail: g.mimanne@yahoo.fr

Article info
Received 29/12/2025; received in revised form 10/2/2026; accepted 10/3/2026
DOI: 10.60923/issn.2281-4485/23727

Abstract
The increasing presence of synthetic dyes in aquatic systems, particularly sunset yellow (SY), has raised urgent concerns due to their toxicity and persistence. In this work, a novel biochar derived from the marine green alga Ulva lactuca was investigated, for the first time, as a sustainable and high-performance adsorbent for SY removal. Comprehensive characterization—including proximate analysis, iodine number (190 mg/g), methylene blue index (59.5 mg/g), point of zero charge (pH_{pzc} = 10.90), zeta potential, FTIR, TGA/DSC, XRF, XRD, SEM, and BET surface area (150.2 m^2/g) revealed a mesoporous structure (pore diameter ≈ 19 nm, IUPAC Type IV) with heterogeneous cavities, low ash and moisture contents, and stable carbon formation. The coexistence of amorphous carbon and mineral phases (KCl, NaCl, SiO_2) was confirmed, providing abundant active sites and enhancing surface interactions. Batch adsorption studies demonstrated exceptional performance, achieving up to 98 % SY removal within only 5 minutes at neutral pH with a low dosage of 0.4 g. These findings highlight Ulva lactuca biochar as a low-cost, eco-friendly, and reusable adsorbent, offering a promising pathway for rapid and efficient remediation of dye-contaminated water.

Keywords: *Adsorption mechanism, mesoporous structure, surface functional groups, reusability cycles, water purification, environmental remediation.*

Introduction

The contamination of aquatic systems by synthetic dyes from various industrial effluents - such as textiles, paper, leather, printing, pharmaceuticals, rubber, pesticides, varnish, petrochemicals, electroplating, food, cosmetics, and plastics - has become a serious environmental concern due to the toxicity, carcinogenicity, and mutagenicity of these compounds. Among these dyes, azo dyes are the most commonly used, with sunset yellow FCF (also known as Yellow 6, E110, or SY) being one of the widely applied additives in the food and beverage industries (Banaei et al., 2018; Abbasi, 2017; Satheesh et al., 2016). SY imparts a yellow-orange hue and is frequently added to fruit juices, candies, dairy products, jelly sweets, and soft drinks to enhance color stability and uniformity during production and storage. In addition to its coloring properties, SY is favored for its low production cost, high resistance to light, oxygen, and pH variations, and its ability to reduce microbial contamination. Despite these advantages, excessive intake of SY has been associated with various health risks, including hyperactivity, allergies, nasal congestion, abdominal pain, diarrhea, chromosomal damage, and even tumor development. The acceptable daily intake (ADI) for SY has been limited to 0-2.5 mg/kg body weight by health authorities (Aliabadi and Mahmoodi, 2018) SY is a monoazo dye characterized by sulfonic acid groups and aromatic rings, which confer high chemical and thermal stability, but also make it difficult to degrade in the environment

DOI: 10.60923/issn.2281-4485/23727

(Lima et al., 2019). Its resistance to biodegradation and strong structural symmetry necessitate the development of effective and low-cost removal techniques. Among the available methods, adsorption is considered one of the most efficient, simple, and economical technologies for dye removal from aqueous media. In this context, biochar has gained increasing attention as a low-cost, renewable, and efficient adsorbent. Biochar is a carbon-rich material produced via pyrolysis or gasification of biomass, and is typically endowed with a highly porous structure, large surface area, and a variety of functional groups that promote strong interactions with organic pollutants. Its physicochemical properties - such as pore structure, surface chemistry, particle size, and ash content - can be tailored for optimal adsorption performance (Balajii and Niju, 2019; Chi et al., 2020). Moreover, biochar is biodegradable, thermally and chemically stable, reusable, and environmentally benign. However, biochar production also poses challenges, including high energy requirements, the need for emission control during pyrolysis, and the potential formation of toxic by-products such as polycyclic aromatic hydrocarbons, dioxins, and furans. Overcoming these limitations through optimized synthesis strategies is crucial for advancing biochar applications in water remediation. This study presents a novel and energy-efficient approach by using *Ulva lactuca*, a green macroalga harvested from the Algerian Mediterranean coast, to produce biochar via carbonization at 600 °C for just one hour - a significant reduction in processing time compared to traditional methods. To the best of our knowledge, this is the first report on the use of this marine biomass for the adsorption of sunset yellow dye. The synthesized biochar was thoroughly characterized and applied for SY removal under various operational conditions. Furthermore, its reusability was assessed, revealing high adsorption efficiency over multiple cycles. These findings demonstrate the potential of Ulva lactuca-based biochar as a sustainable and eco-friendly material for the treatment of dye-contaminated water, contributing to the valorization of marine biomass in environmental applications.

Materials and methods

Preparation of biochar

This study focused on the adsorptive properties of the Mediterranean green alga Ulva lactuca, collected from Ain Temouchent, located in northwestern Algeria. The algae were thoroughly washed with distilled water, sun-dried, then ground using a laboratory mill. The resulting powder was sieved using a Retsch AS 200 sieve to obtain particles with a diameter of 63 µm, which were used in the subsequent laboratory experiments. The carbonization step was carried out as follows: approximately 25 g of Ulva lactuca were placed in pre-weighed glass crucibles and carbonized in a muffle furnace (Nabertherm) at 600 °C for 1 hour in the absence of oxygen. The resulting powdered biochar was stored in airtight containers and used as needed.

Adsorbate and analytical method

According to the Standard Methods for the examination of Water and Wastewater, the absorbance of Sunset Yellow SY solution was measured using a UV-visible spectrophotometer at 480 nm. Sunset Yel-low SY, with the molecular formula $C_{16}H_{10}N_2Na_2O_7S_2$, color index 15985, and molecular weight of 452.4 $g{\cdot}mol^{-1}$, exhibits a maximum absorption peak at 480 nm. The concentration and removal rate of SY were determined based on the calibration curve established from the relationship between SY concentration and its absorbance (de Sá et al., 2013; Zhang et al., 2020; Lopes et al., 2021; Sharma et al., 2021).

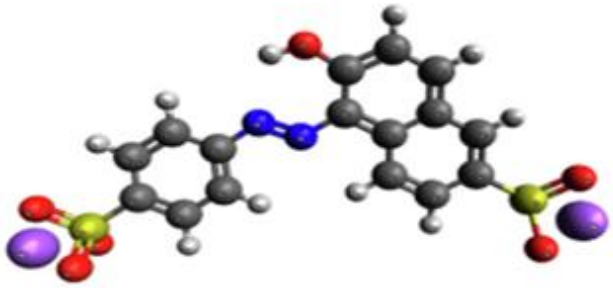

Figure 1. *Molecular structure of sunset yellow, (Zhang et al., 2020)*

Characterization of biochar

The iodine number, methylene blue number, moisture content, and ash content of the biochar were determined using standard methods (ASTM, 2000; Adekola and Adegoke, 2005; Abbas and Darweesh, 2016) . The chemical functional groups present on the biochar surface before and after SY adsorption were identified by Fourier transform infrared spectroscopy (FTIR) using a PerkinElmer spectrometer equipped with a Universal ATR sampling accessory. The surface elemental composition of the biochar was analyzed by X-ray fluorescence (XRF) using a SCIAPS X200 analyzer. The crystalline structure of the green algae before and after carbonization was investigated by X-ray diffraction (XRD) with an HTK 1200N versatile diffractometer. The microstructure of the biochar before and after SY adsorption was examined by scanning electron mi-

DOI: 10.60923/issn.2281-4485/23727

croscopy (SEM) using a HITACHI TM1000 microscope. The zeta potential of the biochar was measured with a Malvern Zetasizer, and the point of zero charge (pHpzc) was determined following standard procedures (Bhuyan and Luukkonen, 2024; Eniola et al., 2023; Ramath et al., 2023; Yang et al., 2023; Mariah et al., 2023). Thermal behavior was evaluated by thermogravimetric and differential scanning calorimetry (TGA/DSC) using an SDT Q600 TA analyzer to assess multistep decomposition and carbonization stability. The textural properties (specific surface area, pore size distribution, and pore volume) of the biochar were determined by nitrogen adsorption-desorption isotherms using a Micromeritics ASAP 2020 Plus (Version 2.00, Serial #3197). Measurements were carried out at liquid nitrogen temperature (−196.19 °C) with a sample mass of 0.1540 g, an equilibration interval of 5 s, and pore structure evaluation based on the BET and BJH methods.

Adsorption study

For the study of the influence of biochar mass on the elimination of SY dye, a 50 mL solution (50 mg/L concentration) of SY dye was added to different masses, from 0.1 to 0.5 g, of biochar with a stirring time of 60 min.The method used to study the influence of pH on the elimination of SY dye is as follows: 0.1 mol/L solutions of NaOH and HCl were prepared to adjust the pH range from 2 to 10 of SY dye solutions at a concentration of 50 mg/L. A volume of 50 mL of the dye at different pH values was added to 0.4 g of biochar and agitated for 60 min. The optimization of the influence of contact time was carried out by mixing 0.4 g of biochar with 50 mL of SY dye solutions at concentrations ranging from 50 to 200 mg/L, under different agitation times from 5 to 60 min. After filtration, the absorbance values of the residual dye were measured using UV spectrophotometry. Another parameter, the effect of temperature, was examined by adding 50 mL of a 50 mg/L SY dye solution to 0.4 g of biochar. The mixture was then agitated for 5 min at different temperatures ranging from 5 °C to 85 °C, adjusted using a thermostatic water bath. In addition, the effect of stirring speed on SY dye adsorption was studied by setting the reaction conditions to 50 mL of SY dye solution at 50 mg/L concentration, 0.4 g of adsorbent, a temperature of 25 °C, and varying the stirring speed from 100 to 600 rpm. Following each experiment, the mixture was filtered through filter paper, and the filtrate was measured to determine the residual concentration of SY dye using a UV-VIS spectrophotometer (PerkinElmer) at a λ_{max} of 480 nm. The batch equilibrium method was used to study the removal of SY on biochar by measuring the absorbance of the dye solution before and after treatment. Based on Equation [1], the removal rate of the dye at equilibrium was calculated (Nguyen et al., 2021):

$$\text{Dye removal } (D_R) = \frac{C_0 - C_1}{C_0} * 100 \qquad [1]$$

where: C_0 and C_t are the concentrations of SY at the start of the experiment and at the time of sampling, respectively.

Results and Discussion

Biochar characterization

Table 1 shows the physical properties and chemical adsorption characteristics of the green algae-based biochar studied.

Ash content , %	32.85
Moisture content, %	3,58
Iodine number, mg/g	190,11
Methylene blue number, mg/g	59,73

Table 1. *Physical properties and chemical adsorption characteristics of the green algae-based biochar studied*

Biochar prepared from the green alga Ulva lactuca carbonized at 600 °C exhibits textural and chemical characteristics consistent with those of marine biochars reported in recent literature. The ash content is relatively high, a consequence of the mineral richness of marine algae. Recent studies report rates of 30-70 % for algal biochars, much higher than those observed for lignocellulosic biomasses (< 10%) (Chen et al., 2023; Shoaib et al., 2024). While such a content may reduce the proportion of carbon surface available for physical adsorption, it nevertheless provides mineral sites (Ca, Mg, K, Si) capable of generating basic and ionic groups (carbonates, phosphates, sulfates), which actively participate in electrostatic interactions with anionic dyes such as sunset yellow (Deng and Su, 2025).

Biochar has a low moisture content (<5 %), which indicates good storage stability and limits the effects of competition with water molecules during adsorption. This result is consistent with the work of (Akmil-Bas and Köseoğlu, 2015), who showed that biochars with a moisture content below 5 % retain a stable internal structure and better adsorption efficiency in aqueous

DOI: 10.60923/issn.2281-4485/23727

media (Nabil et al., 2015; Giusto et al., 2022; Zhang et al., 2022). The measured iodine value (390 mg/g) reflects limited microporosity (0-2 nm). Generally, values between 500 and 1200 mg/g are characteristic of activated carbons, associated with a specific surface area of 900-1100 m^2/g (Saka, 2012; Mopoung et al., 2015; Albatrni et al., 2022). The result obtained therefore confirms that *Ulva lactuca* biochar is not highly microporous, which can be attributed to the absence of activation processes, partial destructuring of pore walls and conversion of micropores into mesopores at high temperature (Shoaib et al., 2024). The MB index, used as a mesoporosity probe (2-50 nm), gave a value of 59 mg/g, which reveals the predominance of mesopores. This observation is consistent with recent work on algal biochars, which highlights the contribution of mesopores to the adsorption of intermediate-sized organic molecules (Deng and Su, 2025). Furthermore, the low affinity of biochar towards MB is explained by an electrostatic repulsion between the overall positive surface of the material ($pH_{pzc} \approx 10.9$) and the cationic dye, as already reported by (Akmil-Bas and Köseoğlu, 2015). The pHpzc of a solid indicates at which pH of the solution the charge on the surface of the solid is zero (Alobaidi and Alwared, 2023). The curve represents the difference between the initial and final pH of the solution (pHf - pHi) as a function of the initial pH (pHi), which determines it. The intersection of the resul ting curve with the horizontal axis passing through the origin gives the value of pHpzc (Figure 2(a)). For this biochar, we find a pHpzc equal to 10.9, which estimates that the adsorbent's surface charge is positive for a pH value lower than 10.9 (H^+) and negative (OH^-) in the opposite case. A high pHpzc of 10.9 suggests the presence of positively charged functional groups (or amine groups) on the surface of the biochar (Vito et al., 2024). These functional groups may come from the compounds present in the marine green algae used to prepare the biochar. However, amine groups are generally basic and may explain why the biochar surface becomes positively charged at pH less than this value (Xiu et al., 2023). Finally, we deduce that for a better adsorption of an anionic dye like SY, it is preferable to work at a pH range from 2 to 10. To understand the surface charge of the biochar prepared from green algae, zeta potential analysis of the particles was carried out. As shown in Figure 2(b), the zeta potential values when the pH is between 2 and 12 are 5.86, 7.74, 22.6, 17.03, -1.02 and -1.98 mV. It can be seen that the particles were positively charged in the pH range between 2 and 10 of the zeta potentials, indicating that biochar has a high SY adsorption capacity through the electrostatic interaction between adsorbent and adsorbate (Obayomi et al., 2023). The thermogravimetric (TGA) and differential scanning calorimetry (DSC) analyses of Ulva lactuca biochar provide valuable insights into its thermal stability and decomposition behavior (Balajii and Niju, 2019; Chi et al., 2020) (Figure 3). The TGA curve reveals four distinct weight-loss stages. The initial loss below ~120 °C corresponds to the evaporation of physically adsorbed moisture (~3–5 %), consistent with the low moisture content determined by proximate analysis. The second stage, between ~200 and 300 °C, is attributed to the

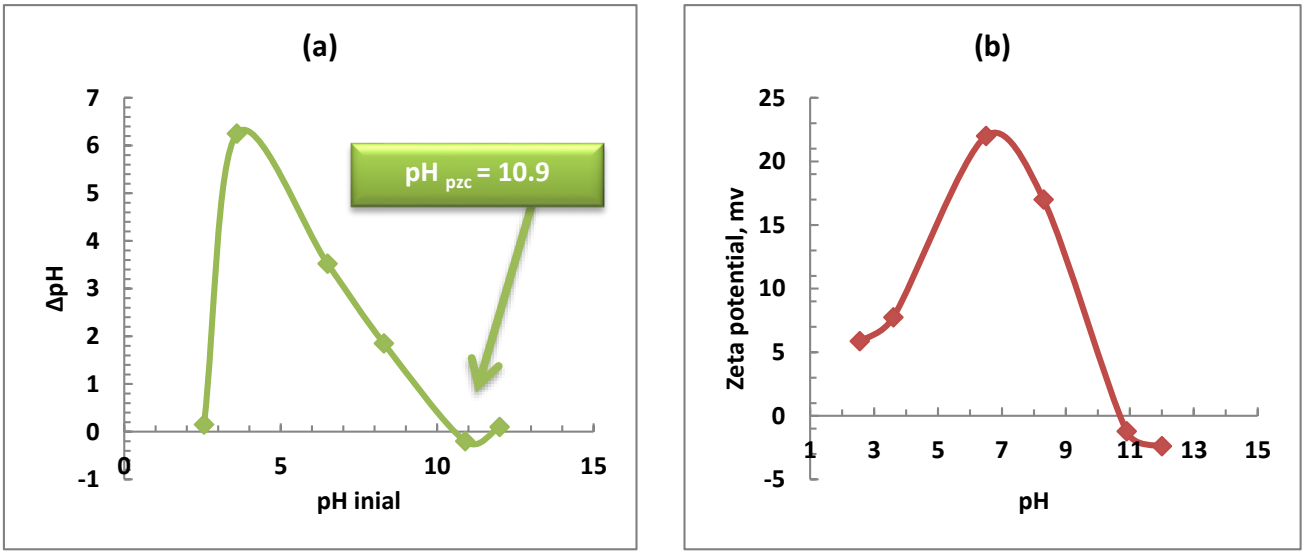

Figure 2. *(a) Point of zero charge of Biochar, (b) Zeta potential analysis of biochar*

EQA 73 (2026): 1 - 12

DOI: 10.60923/issn.2281-4485/23727

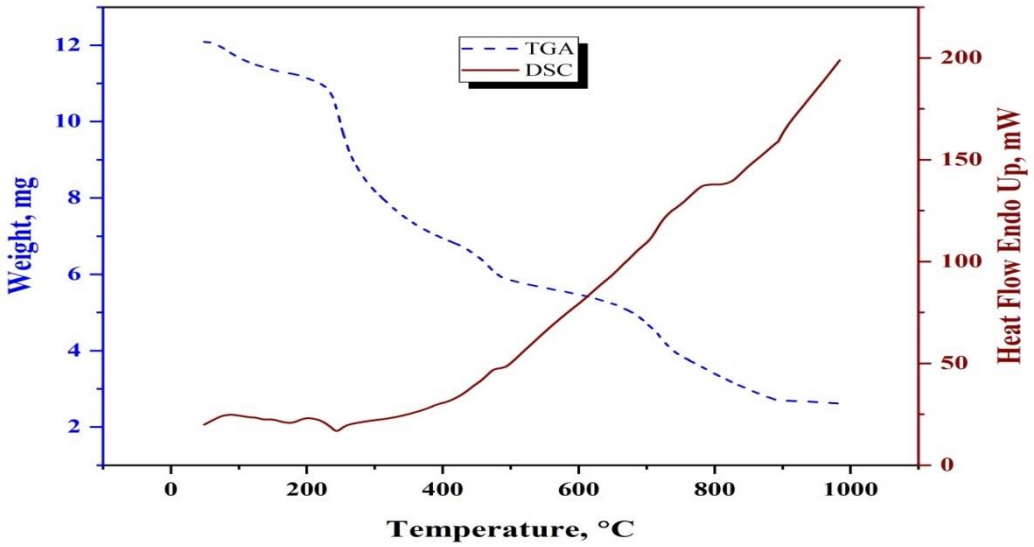

Figure 3
Combined thermogravimetric and calorimetric study (TGA/DSC) of green algae biomass

decomposition of hemicellulose and low-molecular-weight compounds, as evidenced by a moderate exothermic peak in the DSC curve. The third and most significant degradation phase occurs between 300 and 450 °C, mainly due to cellulose depolymerization and volatilization of proteins and lipids, accompanied by sharp exothermic signals, indicating the release of condensable gases (e.g., acetic acid, methanol) and non-condensable gases (CO_2, CH_4, H_2) (Balajii and Niju, 2019; Chi et al., 2020). Beyond 450 °C and up to 600 °C, lignin degradation and secondary char formation take place gradually, with the DSC curve showing overlapping endo- and exothermic features characteristic of complex polymer breakdown. Above 600 °C, the weight loss slows markedly, and the curve stabilizes beyond ~900 °C, leaving a substantial residual mass (~30–35 %), corresponding to fixed carbon and thermally stable mineral phases (carbonates, silicates, and chlorides). This high residual yield confirms the inherently mineral-rich nature of marine algae biochars, in agreement with recent studies (Shoaib et al., 2024; Deng and Su, 2025). The stability of the carbona-ceous fraction above 600 °C suggests that the prepared biochar possesses durable aromatic structures and mi-

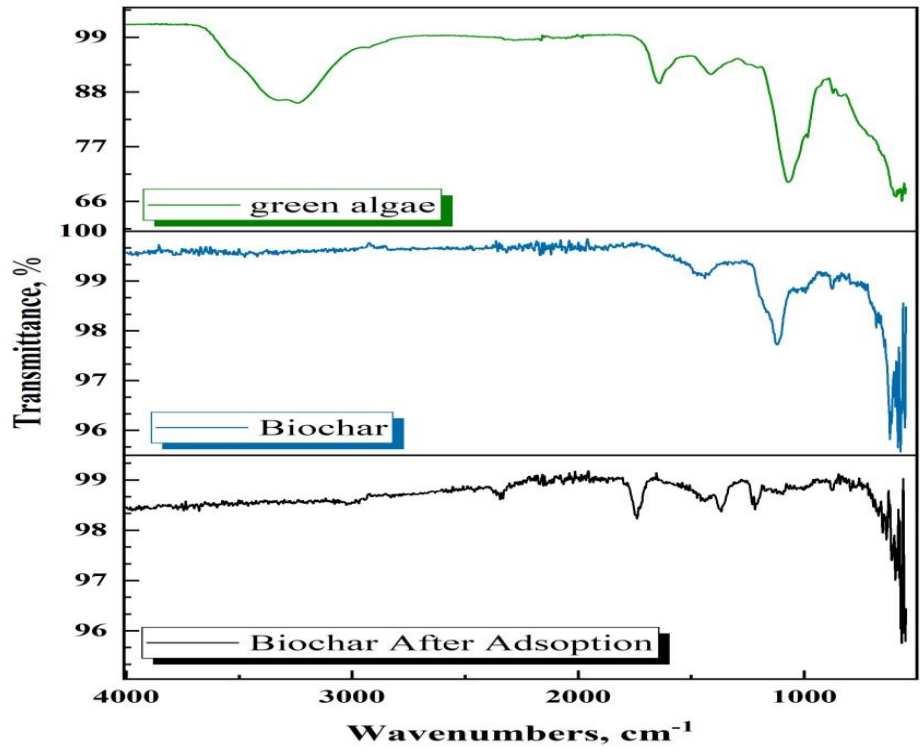

Figure 4
FTIR spectrums of green algae and biochar before and after adsorption

DOI: 10.60923/issn.2281-4485/23727

Table 2. *Modification of functional groups in raw algae and biochar evidenced by FTIR before and after adsorption*

Wavenumber region, cm^{-1}	Raw algae	Biochar	Biochar after adsorption	Assignment / Role
~3400	Intense OH/NH band	Attenuated	Reinforced	OH/NH stretching; H-bonding with -SO_3^- groups
2920-2850	Aliphatic C-H	Disappeared	—	Loss of aliphatic chains during carbonization
1730	C=O esters/acids	Weak	Slight shift	Possible involvement of carbonyl groups in adsorption
1650-1600	Aromatic C=C, amides	Weak band	Reinforced	π-π stacking with Sunset Yellow molecules
1250-1050	C-O-C, S=O, Si-O	Mineral signals persist	Intensified	Sulfonate groups from dye; interaction with mineral matrix
875-800	Si-O / carbonates	Present	Present	Mineral phases acting as ionic adsorption sites

neral support, which are advantageous for adsorption applications, particularly under repeated regeneration cycles. The FTIR spectra of raw green algae, biochar, and biochar after adsorption (Figure 4) provide clear evidence of structural transformations during pyrolysis and subsequent dye adsorption. The raw algae spectrum displayed a broad band at ~3400 cm^{-1} assigned to O-H and N-H stretching (hydroxyls, water, amides), bands at 2920–2850 cm^{-1} corresponding to aliphatic C-H stretching, a strong absorption at ~1730 cm^{-1} from ester/carboxylic C=O vibrations (hemicellulose), a band at 1650–1620 cm^{-1} from aromatic C=C and amide I, and multiple bands between 1250–1050 cm^{-1} indicating C-O-C polysaccharides and sulfate groups, together with signals around 875–800 cm^{-1} attributed to Si-O or mineral salts ($CaCO_3$, KCl). After carbonization, most labile organic functionnal groups disappeared (O-H, C-H, C=O), while the bands in the 1050–1000 cm^{-1} region became more pronounced, confirming the persistence of Si-O and S=O vibrations and the formation of a condensed aromatic carbon matrix (Mariah et al., 2023). Following Sunset Yellow adsorption, significant spectral changes were observed: reappearance and strengthening of the O-H/N-H band at ~3400 cm^{-1}, indicating hydrogen bonding between the biochar surface and dye molecules, enhancement of the aromatic band at 1650–1600 cm^{-1}, suggesting π-π stacking between the biochar's aromatic domains and the dye's azo-aromatic rings, and the emergence/intensification of bands at 1250–1050 cm^{-1}, characteristic of sulfonate S=O stretching, providing direct evidence of dye binding (Deng and Su, 2025). These modifications confirm that adsorption involves a combination of electrostatic interactions (positive biochar surface, pHpzc ≈ 10.9, with -SO_3^- groups), hydrogen bonding, π-π interactions, and mineral-mediated ion complexation (Ca^{2+}, Mg^{2+}, K^+), consistent with recent findings on algae-derived biochars (de Sá et al., 2013; Deng and Su, 2025; Obayomi et al., 2023; Heacock and Marion, 1956). Overall, FTIR analysis demonstrates both the chemical transformation of *Ulva lactuca* into a func-tional carbon matrix and the multifaceted interactions governing sunset yellow adsorption. The X-ray dif-fraction (XRD) patterns of raw *Ulva lactuca* and its derived biochar are shown in Figure 5. The raw algae exhibit broad, low-intensity peaks with crystalline reflections mainly at 2θ ≈ 28, 31, 40, 45 and 50°, which can be assigned to sylvite (KCl) and halite (NaCl) mineral phases, reflecting the natural mineral richness of marine biomass. The relatively diffuse background indicates the presence of amorphous organic matter associated with cellulose, hemicellulose, and lignin. After carbonization at 600 °C for 1 h, the XRD profile of the biochar changes significantly. The crystalline peaks corresponding to mineral phases (e.g., KCl, NaCl, $CaCO_3$, and SiO_2) become sharper and more intense, suggesting the concentration and recrystal-lization of inorganic salts during thermal treatment. In contrast, the broad amorphous hump observed around 2θ = 20–25° corresponds to the disordered carbon structure, confirming the transformation of lignocel-lulosic components into an amorphous carbon matrix. Such amorphous nature is favorable for adsorption be-cause it provides defect sites and enhances surface reactivity. The persistence of crystalline mineral phases also suggests potential contributions to ion exchange and electrostatic interactions with dye molecules. These results are consistent with previous studies on algae-derived biochars, which reported the coexistence of a-

DOI: 10.60923/issn.2281-4485/23727

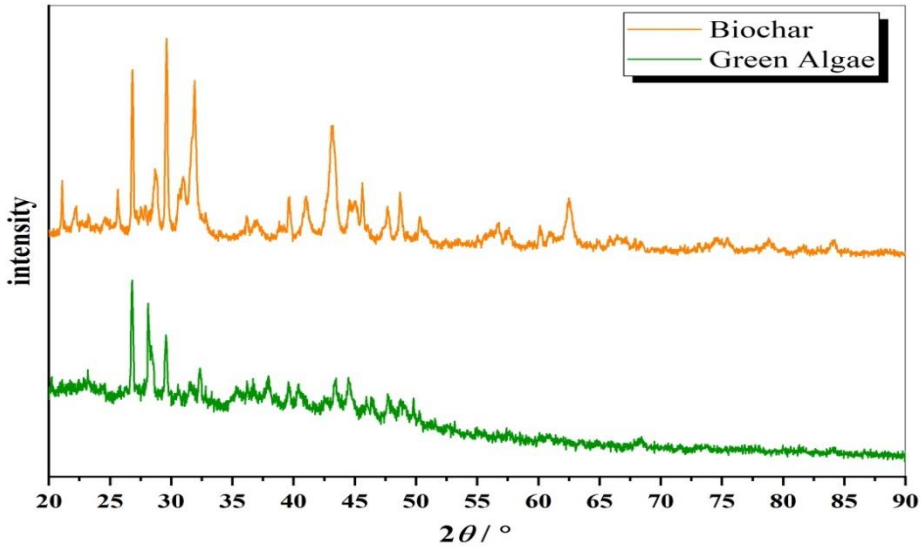

Figure 5
XRD pattern of green algae before and after carbonization

morphous carbon and crystalline minerals after pyrolysis (Shoaib et al., 2024; Alchouron et al., 2020; Armynah et al., 2018; Mahmoud et al., 2020). The elemental composition of the biochar obtained at 600 °C was determined by XRF analysis (Table 3). The results indicate that light elements (C, O, H) account for 53.27 wt.%, confirming the preservation of a carbon-rich structure after carbonization. In addition, more than 40 wt.% of the sample consists of mineral salts such as Mg, Ca, K, and Si, inherited from the marine origin of Ulva lactuca. These minerals are characteristic of algae-derived biochars and have been reported to play a dual role: while they may occupy part of the pore volume, potentially reducing specific surface area, they also enhance the surface chemistry by providing reactive functional groups (-OH, -COOH, -PO_4^{3-}, -SO_4^{2-}) and ionic species that can participate in adsorption processes (Chen et al., 2023). In this study, the high mineral fraction did not hinder the adsorption of Sunset Yellow; instead, it facilitated electrostatic interactions and complexation through carboxyl, phosphate, and sulfate groups, as well as cation bridges involving Ca^{2+}, Mg^{2+}, and K^+. This synergistic effect between the carbon matrix and mineral phases enhances the overall adsorption efficiency and supports the reusability of the biochar as a low-cost adsorbent for dye removal, consistent with recent findings on mineral-rich biochars (Akmil-Bas and Köseoğlu, 2015). The SEM micrograph of the biochar obtained by carbonization at 600 °C (Fig. 6a), magnification scale: 500 µm revealed a heterogeneous surface morphology characterized by a rough texture with irregular cavities and pores of varying sizes. Such morphological features are beneficial for adsorption, as they increase surface roughness and provide accessible channels for the diffusion and retention of adsorbate molecules (Shoaib et al., 2024). The presence of abundant pores of different dimensions is consistent with the BET results, which indicated a mesoporous structure, and further supports the suitability of *Ulva lactuca* biochar as an efficient adsorbent. After adsorption of Sunset Yellow (Fig. 6b), scale: 500 µm, the surface morphology underwent a marked change. The initially porous and rough surface appeared partially covered by adsorbed dye molecules, and agglomerated particles could be observed, confirming the deposition of Sunset Yellow on the biochar surface. Moreover, the distribution of functio-

Table 3. *The main elements and their weight percentage in biochar*

Element	Content, wt.%
Light Elements (C, O, H)	53.27 ± 0.000
Mg	11.65 ± 0199
S Sulfur	10,87 ± 0,023
Ca Calcium	8,04 ± 0,015
K Potassium	8,00 ± 0,016
Si Silicon	4,61 ± 0,037
P Phosphorus	0,246 ± 0,007
Al Aluminum	1,49 ± 0,043
Cr Chromium	0,035 ± 0,004
Ti Titanium	0,192 ± 0,016
Fe Iron	1,48 ± 0,015
Mn Manganese	0,033 ± 0,003
Ni Nickel	0,003 ± 0,001
Cu Copper	0,003 ± 0,000
Zn Zinc	0,005 ± 0,000
Rb Rubidium	0,009 ± 0,000
Zr Zirconium	0,035 ± 0,000
Sr Strontium	0,036 ± 0,000

DOI: 10.60923/issn.2281-4485/23727

Table 4. *Textural properties of the algae-derived biochar*

Sample	Specific surface area, $m^2\ g^{-1}$	Pore volume, $cm^3\ g^{-1}$	Average pore diameter, nm	Isotherm type	Dominant porosity
Biochar	150.2	0.0082	19.0	Type IV (IUPAC)	Mesoporous (15-25 nm)

nal groups and dye residues on the outer surface suggests that adsorption occurred mainly via electrostatic interactions between the negatively charged sulfonate groups of Sunset Yellow and the positively charged surface sites of the biochar (pHpzc ≈ 10.9). These observations are in agreement with the FTIR analysis, which revealed the appearance of sulfonate bands after adsorption, and with recent literature highlighting the synergistic role of biochar morphology and surface charge in the adsorption of anionic dyes (Alchouron et al., 2020). BET (Brunauer-Emmett-Teller) analysis of *Ulva lactuca* biochar reveals a mode-rate specific surface area of 150.2 m^2/g, associated with a total pore volume of 0.0082 cm^3/g and an average pore diameter of approximately 19 nm, characteristic of a mesoporous structure (IUPAC type IV isotherm, with hysteresis). This result is consistent with the relatively low iodine value (390.11 mg/g), which reflects li-mited microporosity (0-2 nm), and confirms the absence of strong physical or chemical activation. In contrast, the methylene blue value (59 mg/g) highlights the preponderance of mesopores (2-50 nm), favorable to the diffusion of medium-sized organic molecules such as dyes. The developed mesoporosity plays a key role in adsorption kinetics by facilitating the transport of molecules to the active sites, while the surface chemistry (oxygenated groups, basic minerals, etc.) mainly governs the interaction mechanisms. This synergy explains why, despite reduced microporosity, biochar exhibits high adsorption efficiency for Sunset Yellow, an anionic dye with dimensions compatible with the size of the mesopores.

Optimization of process parameters and validation of experimental results

The quantity of adsorbent is an essential parameter in adsorption studies because it offers a larger adsorption surface, which can lead to an increase in the adsorbed quantity of the pollutant (Zhao et al., 2023). For this, the mass of the biochar was varied between 0.1 and 0.5 g, and the other parameters were fixed: contact time 60 min, pH of dye solution, temperature 25 °C, and initial concentration 50 mg/L with a 63 µm particle size. Following the filtration process and the measurement of the absorbance, the removal rate was calculated, and the findings are illustrated in Figure 7. The removal rates of SY increased with increasing biochar mass. However, the rate of removal gradually stabilized once a certain amount of biochar had been reached. Increasing the biochar dosage provides a larger specific surface area and more binding sites, which in turn improves the removal effect (Anwar et al., 2010). It is observed that the SY removal increased, ranging from 52 % to 98 %, with the increase in adsorbent mass up to a limit of 0.4 g. This could be explained by the increase in the available sorption surface and the availability of more adsorption sites with increasing amounts of biochar. After 0.4 g, the removal rate gradually stabilized. The amount of 0.4 g was determined to be ideal and set for the other tests.

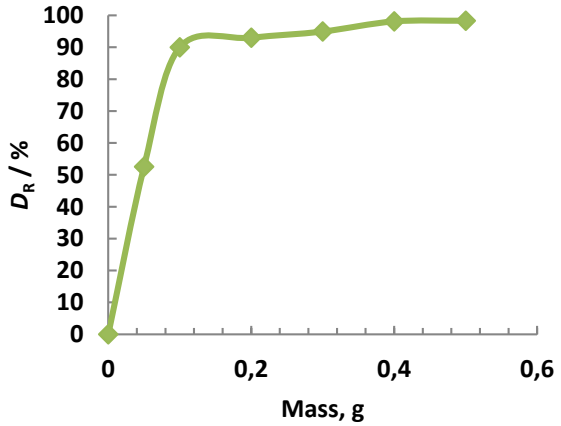

Figure 7. *Effect of biochar mass on the removal of SY dye*

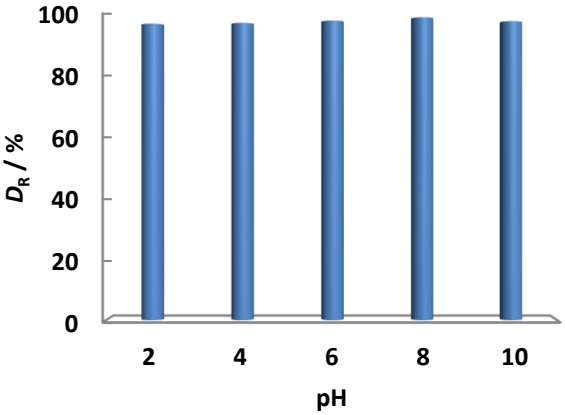

Figure 8. *Effect of pH solution on the removal SY by Biochar*

DOI: 10.60923/issn.2281-4485/23727

The variation in pH of the solution has a major effect on the adsorption process due to the appearance of functional groups and reactive atoms in the structure of adsorbents and adsorbates. For this reason, the influence of pH on the adsorption of SY dye was studied in a pH range between 2 and 10 using an initial SY concentration of 50 mg/L, 60 min contact time, and an adsorbent mass of 0.4 g at 25 °C. It was observed from the results that pH has no significant influence on the ad-sorption of SY on biochar. For all pH values studied, the decolorization of the different SY solutions was al-most complete (Fig. 8). The SY dye has sulfonate groups; therefore, it has one or more negative electric charges in aqueous solutions. At lower pH values, the amine groups of the adsorbent are protonated, and at pH 10.9 the surface has zero net charge, known as pHpzc. It can also be seen that the particles were positively charged in the pH range between 2 and 10, according to the zeta potential, and the sulfonate groups of the SY dye facilitated the electrostatic interaction, which explained the strong adsorption of the adsorbent for SY with 98 % efficiency. Furthermore, the presence of characteristic peaks belonging to the functional groups of Sunset Yellow (SY) in the FTIR spectrum is evidence of the interaction of the SY dye with the functional groups of the adsorbent (Anwar et al., 2010). Figure 9 shows the effect of initial dye concentration on retention rate at different contact times. For the six concentrations used, the retention rate increases with the increase in reaction time, following two different slopes. The first is fast and takes place in the first 5 minutes, while the second is slower and could express the balance between the fractions of dye retained and those desorbed. The overall retention is comparable for the four concentrations, with a yield that decreases as the concentration increases, with orders of magnitude of 98.13, 98, 97.95 and 94.61 % for concentrations of 30, 50, 70, and 100 mg/L, respectively, in the first 5 minutes. After 5 minutes, a saturation level is noticed. Most of the SY dye transferred to the biochar is obtained in the first 30 minutes, with yields of around 93.14 and 88.78 % for concentrations of 150 and 200 mg/L, respectively. After 30 minutes, the formation of the saturation level was again noticed. Additionally, the lower the initial concentration of the dye, the shorter the time required to reach the adsorption equilibrium state. This performance was due to the electrostatic reaction process between the SY dye and the functional groups of the adsorbent, which were gradually saturated (Alobaidi and Alwared, 2023). Figure 10 shows that the higher the reaction temperature, the greater the adsorption rate of SY. However, it is noted that there is no difference in SY elimination between 20 and 85 °C, with an elimination rate of 97 %. The slight increase in SY adsorption with temperature from 5 to 20 °C is due to the addition of energy to SY dye; this energy increases the mobility of the dye and the diffusion rate. It was found that the adsorption of SY increased from 80 % to 97.77 % as the temperature increased from 5 to 85 °C. As demonstrated in Figure 11, the adsorption removal of Sunset Yellow increased by elevating the stirring rate from 100 to 600 tr/min. These stirring rates were determined based on prior research indicating that, at low stirring rates, the adsorbent aggregated at the bottom rather than being distributed throughout the solution, leading to the burial of numerous active sites under the adsorbent layers above (El-Sheekh et al., 2020). Due to the homogeneous su-

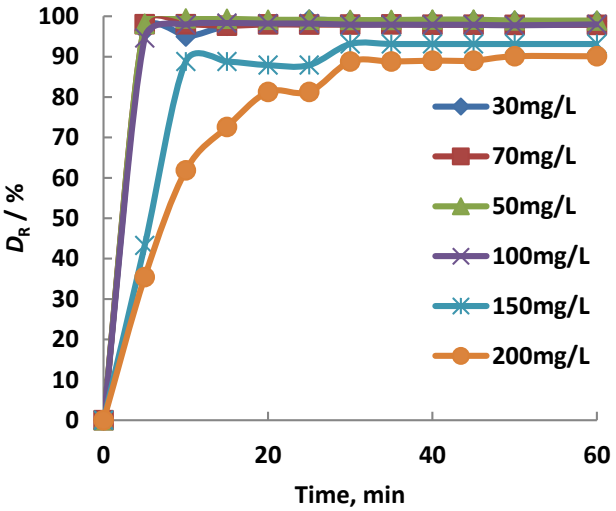

Figure 9. *SY removal by Biochar at various contact times and over different concentrations*

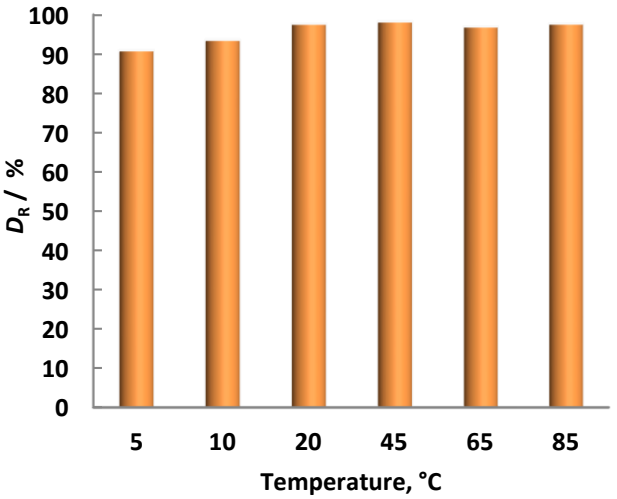

Figure 10. *Effect of temperature on the removal of SY dye*

DOI: 10.60923/issn.2281-4485/23727

spension of the biochar, the adsorption removal of SY also stabilized when the agitation speed was increased from 500 to 600 tr/min. 500 tr/min was thus selected as the best speed for all tests in this study.

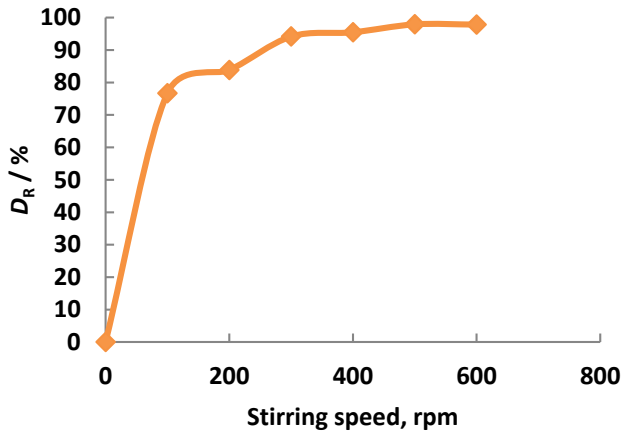

Figure 11. *Effect of stirring speed on elimination of SY dye*

Conclusions

In this study, a biochar derived from the marine green alga Ulva lactuca was successfully prepared through carbonization at 600 °C and investigated as a novel adsorbent for the removal of Sunset Yellow dye. A wide range of characterization techniques (proximate analysis, BET surface area, FTIR, TGA/DSC, XRF, XRD, and SEM) provided a comprehensive understanding of its physicochemical properties. The biochar exhibited a mesoporous structure with a specific surface area of 150 m^2/g, a low moisture content, and a moderate ash fraction enriched in mineral elements (Ca, Mg, K, Si), which not only contributed to structural stability but also introduced additional active sites for adsorption. Thermal analysis confirmed its stability up to 600 °C, while FTIR and XRD analyses revealed the coexistence of amorphous carbon domains and crystalline mineral phases, providing a dual functionality in the adsorption process. Batch adsorption experiments demonstrated that under optimized conditions (0.4 g adsorbent dose, neutral pH, 5 min contact time, 500 rpm, room temperature), the biochar achieved a removal efficiency of 98 %, outperforming several conventional low-cost adsorbents. The adsorption mechanism was mainly governed by electrostatic attractions between the negatively charged sulfonate groups of sunset yellow and the positively charged sites of the biochar, complemented by π-π interactions, hydrogen bonding, and ion exchange facilitated by mineral constituents. Overall, these findings demonstrate that *Ulva lactuca*-derived biochar is a promising, low-cost, eco-friendly, and reusable adsorbent for dye-contaminated water treatment. Its mesoporous structure, mineral-rich composition, and surface chemistry provide a synergistic advantage over conventional biomass-based biochars. Future research should focus on pilot-scale studies, regeneration protocols, and adsorption performance in real industrial wastewater to validate its potential for practical and large-scale applications in sustainable water purification technologies.

Graphical abstract

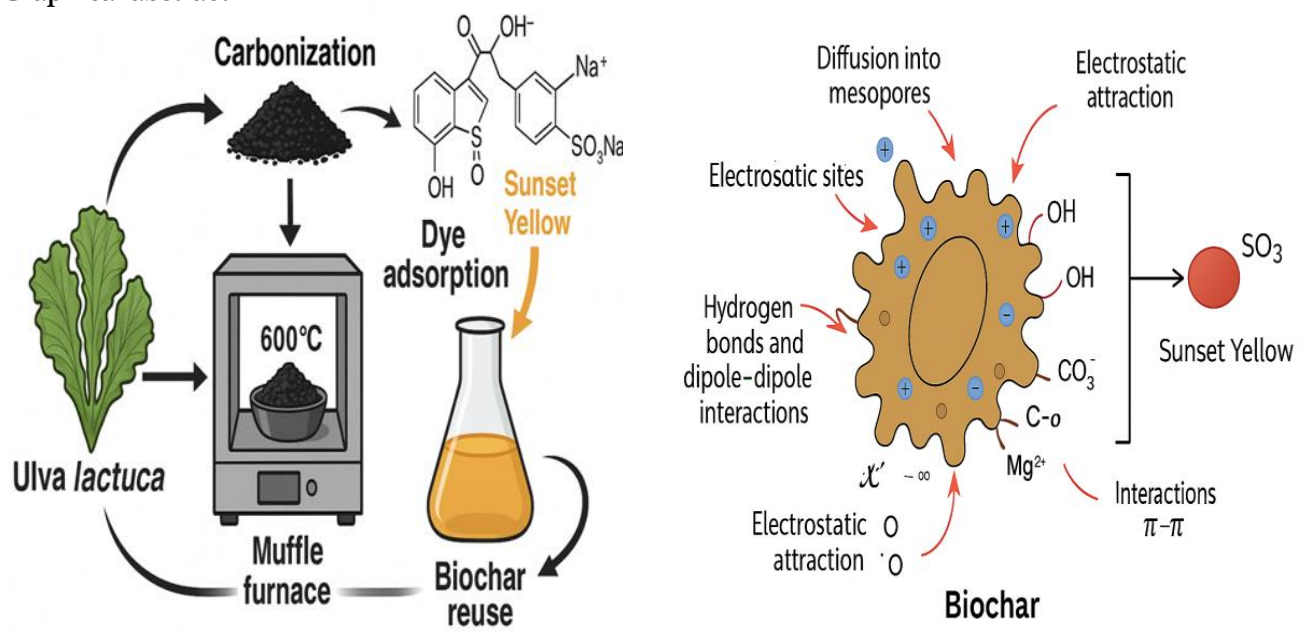

DOI: 10.60923/issn.2281-4485/23727

Acknowledgements
The authors would like to thank the Laboratory of Materials and Catalysis for their support and for providing access to laboratory facilities.

Conflict of Interest
The authors declare no conflict of interest.

References

ADEKOLA F.A., ADEGOKE H.I. (2005) Adsorption of blue-dye on activated carbons produced from rice husk, coconut shell and coconut coirpith. Ife Journal of Science, 7(1):151–157. https://doi.org/10.4314/ijs.v7i1.32169

ABBASI M. (2017) Synthesis and characterization of magnetic nanocomposite of chitosan/SiO_2/carbon nanotubes and its application for dyes removal. Journal of Cleaner Production, 145:105–113. https://doi.org/10.1016/j.jclepro.2017.01.046.

ABBAS A.S., DARWEESH T.M. (2016) Preparation and Characterization of Activated Carbon for Adsorption of Fluoroquinolones Antibiotics. Journal of Engineering, 22(8):140–157. https://doi.org/10.31026/j.eng.2016.08.09

AKMIL-BAS C, KÖSEOĞLU E. (2015) Preparation, structural evaluation and adsorptive properties of activated carbon from agricultural waste biomass. Advanced Powder of Technology., 26:811–818. https://doi.org/10.1016/j.apt.2015.02.006

ALBATRNI H., QIBLAWEY H., AL-MARRI M.J. (2022) Walnut shell based adsorbents: a review study on preparation, mechanism, and application. Journal of Water Process Engineering, 45:102527. https://doi.org/10.1016/j.jwpe.2022.102527.

ALCHOURON J., NAVARATHNA C., CHLUDIL H.D., DEWAGE N.B., PEREZ F., HASSAN E.B., PITTMAN CU J.R,. VEGA A.S., MLSNA T.E. (2020) Assessing South American Guadua chacoensis bamboo biochar and Fe_3O_4 nanoparticle dispersed analogues for aqueous arsenic(V) remediation. Science of Total Environment, 706:135943. https://doi.org/10.1016/j.scitotenv.2019.135943

ALIABADI R.S., MAHMOODI N.O. (2018) Synthesis and characterization of polypyrrole, polyaniline nanoparticles and their nanocomposite for removal of azo dyes; Sunset Yellow and Congo Red. The Journal of Cleaner Production, 179:235–245. https://doi.org/10.1016/j.jclepro.2018.01.035

ANWAR J., SHAFIQUE U., SALMAN M., DAR A., ANWAR S. (2010) Removal of Pb(II) and Cd(II) from water by adsorption on peels of banana. Bioresources Technology, 101:1752–1755. https://doi.org/10.1016/j.biortech.2009.11.041

ARMYNAH B., ATIKA DJAFAR Z., PIARAH W.H., TAHIR D. (2018) Analysis of chemical and physical properties of biochar from rice husk biomass. Journal of Physics Conference Series, 979:012038. https://doi.org/10.1088/1742-6596/979/1/012038 .

ASTM STANDARD. (2000) Standard test method for total ash content of activated carbon. ASTM International, Designation D2866-94. https://doi.org/10.1520/D2866-11

BALAJII M., NIJU S. (2019) Biochar-derived heterogeneous catalysts for biodiesel production. Environmental Chemistry Letters, 17:1447–1469. https://doi.org/10.1007/s10311-019-00885-x

BHUYAN M.A.H., LUUKKONEN T. (2024) Adsorption of methylene blue by composite foams containing alkali-activated blast furnace slag and lignin. International Journal of Environmental Science and Technology, 21:3789–3802. https://doi.org/10.1007/s13762-023-05245-5

BANAEI A., FAROKHI-YAYCHI M., KARIMI S., VOJOUDI H., NAMAZI H., BADIEI A., POURBASHEER E. (2018) 2,2'-(Butane-1,4-diylbis(oxy))dibenzaldehyde cross-linked magnetic chitosan nanoparticles as a new adsorbent for the removal of Reactive Red 239 from aqueous solutions. Materials Chemistry and Physics, 212:1–11. https://doi.org/10.1016/j.matchemphys.2018.02.036

CHEN H., ZHANG Z., LIU Y. (2023) Crystalline and amorphous phase transitions of marine biomass chars: adsorption implications. Bioresource Technology, 368:128353. https://doi.org/10.1016/j.biortech.2023.128353

CHI N.T.L., ANTO S., AHAMED T.S., KUMAR S.S., SHANMUGAM S., MELVIN S. (2020) A review on biochar production techniques and biochar-based catalyst for biofuel production from algae. Fuel, 287:119411. https://doi.org/10.1016/j.fuel.2020.119411

DENG B., SU Y. (2025) Adsorption mechanism in water treatment by biochar and its modified materials: a review. Applied and Computational Engineering, 180:190–199. https://doi.org/10.54254/2755-2721/2026.KA27177

ENIOLA J.O., SIZIRICI B., KHALEEL A., YILDIZ I. (2023) Fabrication of engineered biochar–iron oxide from date palm frond for the effective removal of cationic dye from wastewater. Journal of Water Process Engineering, 54:104046. https://doi.org/10.1016/j.jwpe.2023.104046

EL-SHEEKH M., EL-SABAGH S., ABOU ELSOUD G., ELBELTAGY A. (2020) Efficacy of immobilized biomass of the seaweeds Ulva lactuca and Ulva fasciata for cadmium biosorption. Iranian Journal of Science and Technology, Transactions A: Science, 44:37–49. https://doi.org/10.1007/s40995-020-0085-2

GIUSTO P.R., PANIWNYK L., TAVARES F., FRANÇA A.S., DOTTO G.L (2022) Activated carbon derived from sugarcane and modified with natural compounds for enhanced adsorption of organic pollutants. Scientific Reports,

DOI: 10.60923/issn.2281-4485/23727

12:22421. https://doi.org/10.1038/s41598-022-22421-8

HEACOCK R.A., MARION L. (1956) The infrared spectra of secondary amines and their salts. Canadian Journal of Chemistry,. 34:1782–1795. https://doi.org/10.1139/v56-231

LIMA V.V.C., DALLA NORA F.B., PERES E.C., et al. (2019) Synthesis and characterization of biopolymers functionalized with APTES for the adsorption of Sunset Yellow dye. Journal of Environmental Chemical Engineering, 7:103410. https://doi.org/10.1016/j.jece.2019.103410

LOPES G.K.P., ZANELLA H.G., SPESSATO L. (2021) Steam-activated carbon from malt bagasse: optimization of preparation conditions and adsorption studies of Sunset Yellow food dye. Arabian Journal of Chemistry, 14:103001. https://doi.org/10.1016/j.arabjc.2021.103001

MAHMOUD M.E., ABDELFATTAH A.M., THARWAT R.M., NABIL G.M. (2020) Adsorption of negatively charged food Tartrazine and Sunset Yellow dyes onto positively charged triethylenetetramine biochar. Journal of Molecular Liquids, 318:114297. https://doi.org/10.1016/j.molliq.2020.114297

MARIAH M.A.A., ROVINA K., VONNIE J.M., ERNA K.H. (2023) Characterization of activated carbon from waste tea (*Camellia sinensis*). South African Journal of Chemical Engineering, 44:113–122. https://doi.org/10.1016/j.sajce.2023.01.007

MOPOUNG S., MOONSRI P., PALAS W., KHUMPAI S. (2015) Characterization and properties of activated carbon prepared from tamarind seeds. The Scientific World Journal, 2015:415961. https://doi.org/10.1155/2015/415961

NABIL M.M., AZ M.A., ZAINUL Z.A. (2015) Preparation and characterization of activated carbon from pineapple waste biomass. International Biodeterioration and Biodegradation, 102:274–280. https://doi.org/10.1016/j.ibiod.2015.04.012

NGUYEN X.C., NGUYEN T.T.H., NGUYEN T.H.C. (2021) Sustainable carbonaceous biochar adsorbents derived from agro-wastes. Chemosphere, 282:131009. https://doi.org/10.1016/j.chemosphere.2021.131009

OBAYOMI K.S., LAU S.Y., IBRAHIM O., ZHANG J., MEUNIER L., ANIOBI M.M., ATUNWA B.T., PRAMANIK B.K., RAHMAN M.M. (2023) Removal of Congo Red dye by MOF-decorated biochar. Microporous and Mesoporous Materials, 355:112568. https://doi.org/10.1016/j.micromeso.2023.112568

RAMATH R., SUKUMARAN A.M., RAMACHANDRAN A., BASHEER S.B. (2023) Methyl Orange dye adsorption using iron oxide-incorporated biochar. Bioresource Technology Reports, 22:101470. https://doi.org/10.1016/j.biteb.2023.101470

SAKA C. (2012) BET, TG–DTG, FT-IR, SEM, iodine number analysis and preparation of activated carbon from acorn shell. Journal of Analytical and Applied Pyrolysis, 95:21–24. https://doi.org/10.1016/j.jaap.2011.10.009

SATHEESH R., VIGNESH K., RAJARAJAN M.. (2016) Removal of Congo Red using quercetin modified α-Fe_2O_3 nanoparticles. Materials Chemistry and Physics, 180:53–65. https://doi.org/10.1016/j.matchemphys.2016.05.029

SHARMA S., RANI N.R., VADIRAJ K.T. (2021) Detoxification of Sunset Yellow and Brilliant Blue dyes using soybean peroxidases. Current Research in Green and Sustainable Chemistry, 4:100215. https://doi.org/10.1016/j.crgsc.2021.100215

SHOAIB M., YILMAZ M., EL SIKAILY A. (2024) Algae-derived biochar for dye removal. Scientific Reports, 14:119501. https://doi.org/10.1038/s41598-024-119501

WU Z., WANG X., YAO J., ZHAN S., LI H., ZHANG J., QIU Z. (2021) Synthesis of polyethyleneimine modified CoFe2O4-loaded porous biochar for selective adsorption properties towards dyes and exploration of interaction mechanisms Separation and Purification Technology, 277:119474. https://doi.org/10.1016/j.seppur.2021.119474

XIU L., GU W., SUN Y., WU D., WANG Y., ZHANG H-, ZHANG W., CHEN W. (2023) Fate and supply capacity of potassium in biochar used in agriculture. Science of the Total Environment, 902:165969. https://doi.org/10.1016/j.scitotenv.2023.165969

YANG X., ZHU W., CHEN F., SONG Y., YU Y., ZHUANG H. (2023) Modified biochar prepared from Retinervus luffae fructus. Chemosphere, 322:138088. https://doi.org/10.1016/j.chemosphere.2023.138088

ZHANG L., SELLAOUI L., FRANCO D., DOTTO G.L., BAJAHZAR A., BELMABROUK H., -PETRICIOLET A.B., OLIVEIRA M.L.S., LI Z. (2020) Adsorption of dyes brilliant blue, sunset yellow and tartrazine from aqueous solution on chitosan: Analytical interpretation via multilayer statistical physics model. Chemical Engineering Journal, 382:122952. https://doi.org/10.1016/j.cej.2019.122952

ZHANG Z., LI Y., ZHANG X., et al. (2022) Structural evolution of algae-derived biochar during pyrolysis. Journal of Analytical and Applied Pyrolysis, 164:105532. https://doi.org/10.1016/j.jaap.2022.105532

ZHAO S., WANG X., WANG Q., SUMPRADIT T. KHAN A., ZHOU J., SALAMA E-S., LI X., QU J. (2023) Application of biochar in microbial fuel cells. Ecotoxicology and Environmental Safety, 267:115643. https://doi.org/10.1016/j.ecoenv.2023.115643